Orientation of Cholera Toxin Bound to Model Membranes

Donna Cabral-Lilly,* Gina E. Sosinsky,‡ Robert A. Reed,* Mark R. McDermott,§ and G. Graham Shipley*
*Biophysics Department, Boston University School of Medicine, Boston, Massachusetts 02118, ‡Rosenstiel Center, Brandeis University, Waltham, Massachusetts 02254, and §Department of Pathology, McMaster University, Hamilton, Ontario, Canada L8N 3Z5

ABSTRACT The orientation of cholera toxin bound to its cell-surface receptor, ganglioside G_{M1}, in a supporting lipid membrane was determined by electron microscopy of negatively stained toxin-lipid samples. Image analysis of two dimensional crystalline arrays has shown previously that the B-subunits of cholera toxin orient at the membrane surface as a pentameric ring with a central channel (Reed, R. A., J. Mattai, and G. G. Shipley. 1987. *Biochemistry.* 26:824–832; Ribi, H. O., D. S. Ludwig, K. L. Mercer, G. K. Schoolnik, and R. D. Kornberg. 1988. *Science (Wash. DC).* 239:1272–1276). We recorded images of negatively stained cholera toxin and isolated B-pentamers oriented perpendicular to the lipid surface so that the pentamer ring is viewed from the side. The pentamer dimensions, estimated from the average of 100 molecules, are approximately 60 by 30 Å. Images of side views of whole cholera toxin clearly show density above the pentamer ring away from the lipid layer. On the basis of difference maps between averages of side views of whole toxin and B-pentamers, this density above the pentamer has been identified as a portion of the A-subunit. The A-subunit may also extend into the pore of the pentamer. In addition, Fab fragments from a monoclonal antibody to the A-subunit were mixed with the toxin prior to binding to G_{M1}. Density from the Fab was localized to the region of toxin above the pentamer ring confirming the location of the A-subunit. The structure determined for the homologous heat-labile enterotoxin from *Escherichia coli* shows that the A-subunit lies mostly on one face of this pentamer with a small region penetrating the pentamer pore (Sixma, T. K., S. E. Pronk, K. H. Kalk, E. S. Wartna, B. A. M. van Zanten, B. Witholt, and W. G. J. Hol. 1991. *Nature (Lond.).* 351:371–377). The putative G_{M1} binding sites are located on the opposite face of the B-pentamer. Cholera toxin, therefore appears to bind to a model membrane with its G_{M1} binding surface adjacent to the membrane. Low resolution density maps were constructed from the x-ray coordinates of the *E. coli* toxin and compared with the electron microscopy-derived maps.

INTRODUCTION

Cholera toxin (CTX) is the pathologically active agent secreted by the bacterium *Vibrio cholerae*. The toxin, a member of the enterotoxin family, has an AB_5 arrangement of subunits. Five identical B subunits (CTB) form a pentameric ring (monomer M_r 11, 600) that is responsible for binding the toxin to its cell-surface receptor, ganglioside G_{M1} (G_{M1}). The single A-subunit (CTA) is a disulfide-linked dimer (A_1 M_r 22,000; A_2 M_r 5, 400). After reduction of the disulfide bond, the primary action of the A_1 peptide is to catalyze the transfer of an ADP-ribose group from NAD^+ to the α-subunit of G_s-protein at the cytoplasmic face of the cell membrane. This ADP-ribosylated G_s then continually stimulates adenylate cyclase to produce large amounts of cyclic AMP, ultimately resulting in a net efflux of water and ions from the cell (see Finkelstein (1988) and Moss and Vaughan (1988) for reviews).

It has been proposed that the A_1 peptide crosses the cell membrane to reach the cytoplasmic face. The CTB-pentamer has been shown by electron microscopy (EM) to lie flat on a model lipid surface. The pentamer has a diameter of ~60 Å and a central pore ~20 Å wide (Ludwig et al., 1986; Reed et al., 1987; Mosser et al., 1992). EM studies of the whole toxin indicated that CTA was located in the region of the central pore when CTX was membrane bound (Ribi et al., 1988). Data obtained by photolabeling experiments (Wisnieski and Bramhall, 1981) and by calorimetry measurements and fluorescent labeling (Goins and Freire, 1985) suggest that CTA faces the membrane surface as CTX binds. These data however are not conclusive and contradictory evidence, also using hydrophobic photolabeling, has been reported (Tomasi and Montecucco, 1981). The two proposed orientations of binding suggest different modes of entry for A_1 into the cytoplasm: direct translocation across the cell membrane, or possibly though an endocytic pathway as suggested by some investigators (Janicot et al., 1991; Tran et al., 1987).

The structure of the highly homologous, heat-labile enterotoxin from *Escherichia coli* (LT) has been solved to atomic resolution by x-ray diffraction (Sixma et al., 1991, 1992). Although details of the CTX structure will be different, it is reasonable to expect that the overall topology will be the same for both toxins. The A_1 peptide lies on one face of the LT pentamer, and the A_2 peptide emerges through the other end of the central pore. Biochemical studies have identified four residues in CTB that are important for toxin binding to G_{M1} (DeWolf et al., 1981; Ludwig et al., 1985; Tsuji

Received for publication 1 November 1993 and in final form 19 January 1994.

Address reprint requests to Dr. Donna Cabral-Lilly at the Biophysics Department, Boston University School of Medicine, 80 E. Concord Street, Boston, MA 02118.

Dr. Reed's present address is Pharmacia Biosensor, 800 Centennial Avenue, Piscataway, NJ 08854.

Abbreviations used: anti-CTA Fab, the Fab fragment of a monoclonal antibody directed against the A-subunit of cholera toxin; CTB, B-subunit of cholera toxin; CTA, A-subunit of cholera toxin; CTX, cholera toxin from *Vibrio cholerae*; EM, electron microscopy; G_{M1}, ganglioside G_{M1}; LT, heat-labile enterotoxin from *E. coli*; PC, phosphatidyl choline from egg yolk.

0006-3495/94/04/935/07 $2.00

et al., 1985). Lactose was found to bind at the pentamer side of LT opposite that where the A_1 peptide is located (Sixma et al., 1992). The residues shown to be necessary for toxin binding are located on this face which forms a putative binding cleft for G_{M1}. The distance between this cleft and the A_1 peptide (~30 Å) appears too large for A_1 to face the membrane as the toxin binds.

We have used two-dimensional lipid-layer crystallization and EM to view G_{M1}-bound CTX and CTB perpendicular to the lipid plane. The orientation of CTX on the lipid layer was determined directly from the images, from difference maps between CTX and CTB, and by immunolabeling CTA. Moreover, the EM-derived CTX density map was compared with a map of the LT toxin at similar resolution.

MATERIALS AND METHODS

Sample preparation

Lyophilized CTX and CTB were purchased from Calbiochem (San Diego, CA) and hydrated according to supplier's directions. Egg yolk phosphatidyl choline (PC) was obtained from Sigma (St. Louis, MO), and bovine brain G_{M1} from Calbiochem. Lipids were used without further purification. A monoclonal antibody (class IgG2A) to CTA was prepared as described (Drew et al., 1992). An anti-turnip mosaic virus IgG was used as a control. Fab fragments of anti-CTA and anti-turnip mosaic virus IgGs were produced and isolated using the ImmunoPure Fab preparation kit from Pierce (Rockford, IL). The affinity of the anti-CTA Fab for CTX was confirmed by dot blot analysis.

Arrays of CTX or CTB bound to G_{M1} in a PC lipid layer were formed using the two-dimensional lipid-layer crystallization technique as described by Reed et al. (1987), Ribi et al. (1988), and Mosser and Brisson (1991) with the following modifications. The CTX or CTB concentration was kept constant at 250 μg/ml in 50 mM Tris-HCl, pH 7.5, 200 mM NaCl, 1 mM EDTA, 3 mM sodium azide. 14 μl of the protein solution was placed in each Teflon well. A 1-μl drop of G_{M1}:PC (1:3 w/w) at a total lipid concentration of 0.5 mg/ml in $CHCl_3$ was placed on each well to form the lipid layer. The wells were incubated for 14 h at room temperature. A carbon-coated EM grid was placed on each drop and lifted off after 30–60 s. The specimen was then stained with 1% uranyl acetate. For the antibody binding experiments, CTX was mixed with either anti-CTA Fab or anti-turnip mosaic virus Fab and incubated at room temperature for 2h. Lipid-layer crystallization of the CTX-Fab was then carried out as described.

Electron microscopy and image processing

The grids were viewed on a Philips CM12 TEM at 100kV at ambient temperature, and electron micrographs were recorded under low electron dose conditions at 100,000 ×. Two types of arrays were observed on all grids: two-dimensional crystals comparable to those seen by others (Ludwig et al., 1986; Reed et al., 1987; Ribi et al., 1988; Mosser et al., 1992) and tube-like structures with toxin molecules positioned along the edges and viewed perpendicular to the pentamer plane (side views). The difference in sample preparation between this study and previous ones is the GM1:PC ratio. In combination with the high protein concentration this lipid ratio may be important in getting the tube-like structures to form. Areas of micrographs with clear side views were digitized using an Eikonix Imaging System model 1412 (Bedford, MA) at a 25-μm raster corresponding to 2.5 Å/pixel. Approximately 30–60 tube-like structures were used for image processing for each specimen group.

The SPIDER program package (Frank et al., 1981) was used to align, classify, and average the toxin molecules as follows. Individual toxin molecules with an underlying area of membrane were chosen interactively to form a data set of 300–700 particles for each group. Each windowed image was normalized relative to the average background density of its respective micrograph as described by Frank et al. (1988) to eliminate differences in staining between grids. Each data set was rotationally aligned such that the CTB-pentamers and membranes were in the same orientation. The particles were then translationally aligned so that the peak density for the CTB-pentamer was at the center of each image. This two-step alignment procedure was iterated three times using the global average from the previous alignment pass as reference. Correspondence analysis (Frank et al., 1985) was used to classify each data set into two main groups. The CTB molecules showed a variable degree of stain-induced flattening and were grouped according to the height of the CTB-pentamer (top 25% in group 1). For CTX, the classes were based on those with density directly centered above the CTB-pentamer (group 1) and those with density off-center. This variation may be due to flexibility inherent in the CTA subunit or flexibility induced by staining and drying. For CTX/anti-CTA Fab, those with (group 1) and without bound Fab were separated. The Fab containing group was further divided into those with Fab density mostly to the left or right of CTA. Averages were then computed for group 1 in each data set. Three-dimensional cylindrical averages of CTX and CTB were calculated by assuming an axis of symmetry coincident with the 5-fold axis of the CTB-pentamer. Cylindrical symmetry was enforced by imposing a mirror line perpendicular to the membrane plane, and then calculating the central section (Stallmeyer et al., 1989).

Comparison with LT toxin

The atomic coordinates for heat-labile enterotoxin (LT) were extracted from the Protein Data Bank (Bernstein et al. (1977); entry pdb1lts.ent, Sixma et al. (1991)). The LT coordinates were then rotated to the corresponding side view orientation and projection maps were calculated of LT and the LT pentamer at 20-Å resolution using the CCP4 program series (The SERC (UK) Collaborative Computing Project No. 4, Daresbury Laboratory, Warrington WA 4AD, UK). To model the CTX-Fab-labeled average, the Fab coordinates of an Fab-lysozyme cocrystal were taken from the Protein Data Bank (entry pdb2hfl.ent; Sheriff et al. (1987)) and were used to generate a generic 20 Å-resolution Fab fragment. The Fab map was positioned using the program FRODO (Jones, 1978) so that the antigen binding surface was docked with the A-subunit of LT. The LT and Fab coordinates were then combined and a projection map of the complex side view was calculated.

RESULTS

CTX and CTB

The electron micrographs show two orthogonal projections of CTX and CTB bound to G_{M1} in a lipid layer. The top view reveals the flat face of the pentamer looking down the central pore as described previously (Ludwig et al., 1986; Reed et al., 1987, Mosser et al., 1992). Small tube-like structures are also formed where the toxin, located at the edges of the tube, is in a linear array and is viewed from the side of the pentamer ring perpendicular to the 5-fold axis. Fig. 1 *A* shows an EM image of the CTB-pentamer viewed from the side, a montage of representative CTB molecules and the average of 100 particles. Diffuse density corresponding to the lipid matrix is apparent at the bottom of each windowed area, and the CTB-pentamer is located above this lipid region. There is a small but persistent area of low density between the lipid and CTB-pentamer suggesting that, at least in this model system, the pentamer is not in intimate contact with the lipid layer. The pentamer itself is elliptical in shape with a somewhat flat top and bottom and has dimensions of approximately 60 × 30 Å.

An EM image of CTX bound to G_{M1}, a montage of CTX side views and the average of 100 particles are shown in

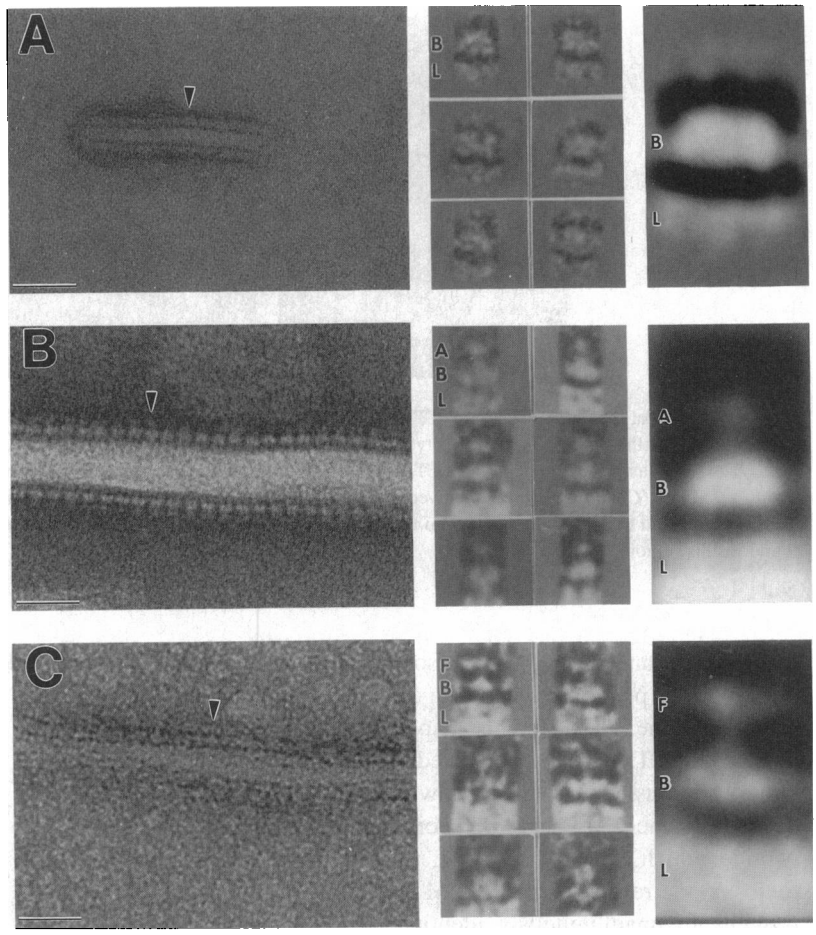

FIGURE 1 Images of cholera toxin bound to G_{M1} in a phospholipid matrix. (*A*) CTB-pentamer. Electron micrograph where the pentamer can be viewed from the side (▼) (*left*); bar = 200 Å. Montage of individual molecules (*middle*). Average of 100 molecules after alignment (*right*). B = CTB-pentamer; L = lipid layer. (*B*) Whole cholera toxin. Electron micrograph with the toxin viewed from the side (▼) (*left*); bar = 200 Å. Montage of individual molecules (*middle*). Average of 100 molecules after alignment (*right*). A = CTA, B = CTB-pentamer, L = lipid layer. (*C*) Whole cholera toxin plus anti-CTA Fab. Electron micrograph where the molecules can be viewed from the side (▼) (*left*) Bar = 200 Å. Montage of individual molecules (*middle*). Average of 80 molecules after alignment (*right*). F = anti-CTA Fab plus CTA, B = CTB-pentamer, L = lipid layer.

Fig. 1 *B*. The lipid layer appears as a diffuse high density band similar to the CTB images. There is again a small region of low density between the lipid and CTX. The CTX density consists of two main domains. One region is near the lipid surface corresponding to the location of the CTB-pentamer. The ellipsoidal shape of the pentamer in the whole toxin average is slightly different than for the pentamer alone. The face adjacent to the membrane is flat, but the opposite face has a more rounded appearance where the second domain begins. The dimensions of the pentamer in CTX are approximately 55 × 35 Å. The second domain is smaller than the pentamer (approximately 30 × 20 Å), is more globular in appearance and is in contact with the pentamer at the top of the central pore. This second smaller domain should correspond to CTA.

Immunolabeling

An Fab fragment from a monoclonal antibody directed against CTA was used to decorate this subunit in the whole toxin. Fig. 1 *C* shows a field of side views of CTX plus anti-CTA Fab, a montage of CTX/anti-CTA Fab complexes and the average of 80 molecules. An Fab fragment from an IgG against turnip mosaic virus was used as a control; no Fab decoration was detected in these specimens (not shown). There was an excess of CTX in the CTX/anti-CTA Fab mixture, therefore, correspondence analysis was used to select those molecules with significant density not found in the CTX average. The extra density in the Fab-containing complexes occurs above the CTB-pentamer and is associated with the smaller density region identified as CTA. The morphology of CTX in the Fab-toxin complex is not significantly different from the CTX image shown in Fig. 1 *B*. Since there is no obvious preferred side orientation of the toxin with respect to the pentamer 5-fold axis, the Fab can be in a number of locations and correspondence analysis was used to distinguish those particles with Fab density lying mostly on the right of CTA and these molecules were used to calculate the average image shown. Anti-CTA Fab density occurring mostly coincident with CTA in this projection will reinforce the CTA density in the average. Although the anti-CTA Fab density is fanned out, it is clear that the Fab decorated only the smaller domain above the CTB-pentamer confirming the original assignment of CTA.

Axial sections

Fig. 2 shows axial sections of the cylindrical averages of CTX and the CTB-pentamer and a difference map between them. For the CTB-pentamer (Fig. 2 *A*), a region of low density corresponding to the central pore is revealed. In the CTX axial section (Fig. 2 *B*), CTA density above the pore

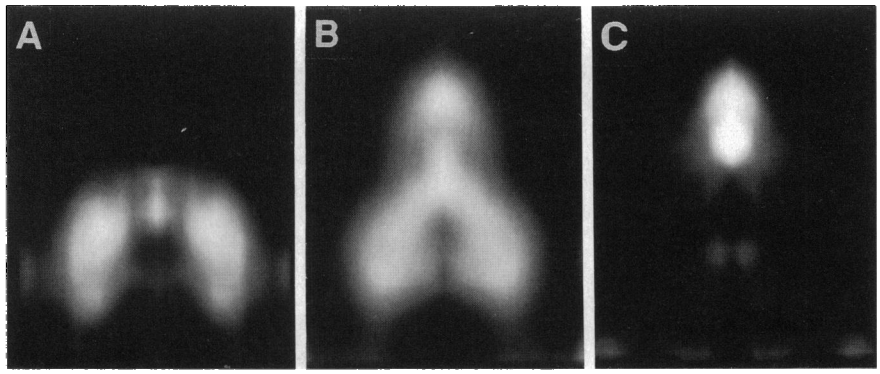

FIGURE 2 Axial sections of CTB and CTX side views. (*A*) Greyscale axial section of CTB-pentamer. The G_{M1}-binding face, which lies adjacent to the lipid matrix, is at the bottom. A low density region is evident in the center of the CTB-pentamer which corresponds to the central pore. (*B*) Axial section of CTX oriented as in *A*. The density of CTA is clearly visible and is connected to the pentamer. The central pore also appears to contain higher density than CTB alone. (*C*) Difference map between CTX and CTB axial sections. Density existing in CTX but not in CTB appears white. The CTA subunit is clearly visible and this density extends into the top of the pentamer pore. Although some low density is seen further into the pore, no significant peaks are found in this region.

is quite clear and strong. There also appears to be increased density in the pentamer pore when compared with the CTB-pentamer alone. The difference map (Fig. 2 *C*) shows that the majority of CTA density is located on one side of the pentamer. There is a small area of low density near the bottom of the pentamer that may correspond to a region of the A_2-peptide which goes through the pore in the *E. coli* LT toxin. At the resolution of the EM maps, however, it is not possible to unambiguously identify the CTX component corresponding to this area.

Comparison of CTX and LT

The averaged images for CTB and CTX were compared with the structure of the homologous LT toxin (Sixma et al., 1991). Fig. 3 shows a comparison of the side view projections. The B-pentamer (Fig. 3 *A*), whole toxin (Fig. 3 *B*), and "Fab-labeled" toxin (Fig. 3 *C*) for CTX (*left*) and LT (*right*) at 25 and 20 Å, respectively, are shown with three contour levels overlaying the greyscale maps. Only positive contours corresponding to protein density are shown with the outermost contour defining the boundaries of the molecules. The overall size, shape, and subunit location are remarkably similar for the two toxins at this resolution. Moreover, except for the Fab regions, the areas of higher contour, i.e., higher density, correspond between the CTX and LT maps. Since the CTX image is a global average of 100 particles in a random orientation with respect to the pentamer 5-fold, the CTA subunit density is lower than would be expected if all CTX molecules were exactly aligned. The Fab bound to CTX is at a lower contour level than the LT-Fab model; this is most probably due to the fanning effect of averaging particles not perfectly aligned with respect to the Fab. The dimensions of CTX and its CTB-pentamer are slightly smaller than LT partially due to the effects of the negative stain.

DISCUSSION

The side view projection of cholera toxin bound to its receptor in a lipid layer provides a unique method to visualize directly the initial binding orientation of the toxin. The individual molecules can be discerned in the linear array with the lipid layer location unequivocal. Moreover, the major difference between the CTB-pentamer and the whole CTX is clear even in the original images. The image averages of 100 particles for each, serve to increase the signal-to-noise and clearly define the morphology of this projection. CTX appears to bind with the A subunit initially facing away from the lipid surface. In the CTX images, each toxin molecule is facing in the same direction. The binding orientation appears to be unique and does not seem to be influenced by protein-protein packing during incubation. The CTA identification was confirmed by immunolabeling with an Fab fragment from a monoclonal antibody directed against this subunit. Although the Fab density was smeared in the averaged image, it was associated exclusively with the toxin density above the CTB-pentamer when bound to G_{M1}.

Axial sections of cylindrical averages of CTB and CTX were used to determine whether a portion of CTA is located in the pentamer pore. The results indicate that the majority of CTA is positioned outside and at the top of the pore with no significant domain going through. In LT, the single helix of the A_2 domain extends through the pore and emerges at the other end (Sixma et al., 1992). It is possible that this occurs for CTX also, and that the density of A_2 was not detectable in the low resolution EM averages.

A comparison of the CTX side view with the homologous LT toxin (Sixma et al., 1991) provided additional evidence for the identification of CTA and the CTB-pentamer, as well as features of the interface between the domains. The superposition of a 20-Å electron density map of LT and a cylindrically averaged CTX model suggests that the overall size

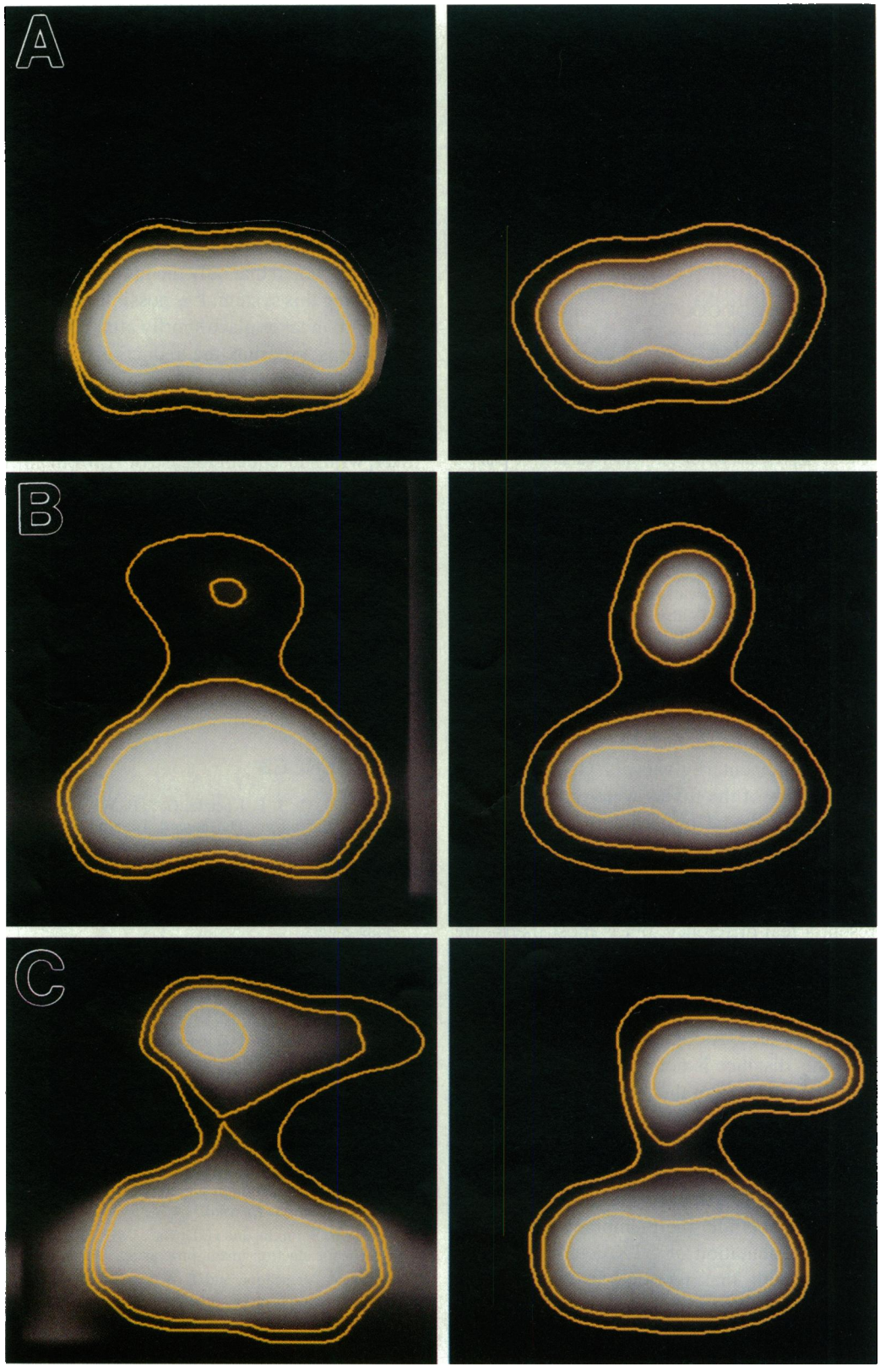

FIGURE 3 Comparison of CTX and LT in projection. Three contour levels are drawn in yellow over the greyscale maps. Only positive contours are shown, with the outermost contour defining the edges of the protein. The contour levels are equally spaced at intervals of one-third the total positive density. (*A*) B-pentamer. (*B*) Whole toxin. (*C*) Whole toxin with Fab-labeled A-subunit. The left column shows the averaged images of cholera toxin at approximately 25 Å-resolution. The right column shows the corresponding projection of LT at 20 Å-resolution.

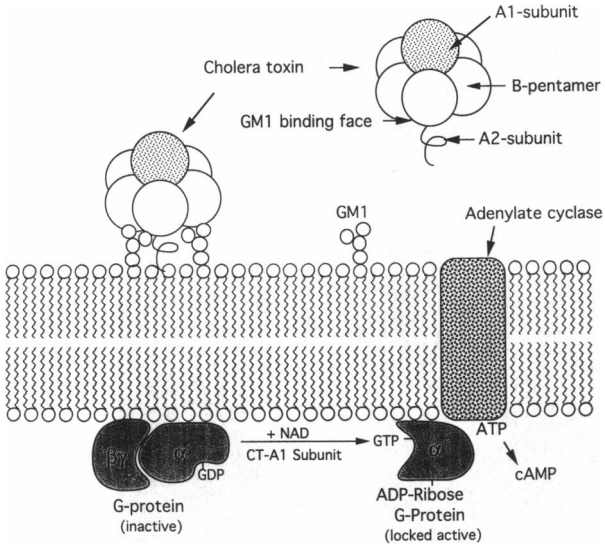

FIGURE 4 Schematic representation of the initial binding of cholera toxin to a cell membrane. The toxin is a complex of a pentamer of B-subunits with the A_1-peptide located one one face of the pentamer and the A_2-peptide extending through the pentamer pore. The G_{M1}-binding sites are on the pentamer face opposite to where the A_1-peptide is located. The toxin initially binds to the cell with its G_{M1}-binding sites adjacent to the lipid membrane. The catalytic activity of the A_1-peptide occurs at the cytoplasmic side of the plasma membrane. The A_1-peptide must either translocate across the lipid bilayer after reduction of the A_1-A_2 disulfide bond at the cell surface, or be directed back to the plasma membrane through an endocytic pathway.

and subunit position are similar for the two enterotoxins (data not shown). This complementarity was also apparent when the side view projections of the toxins were compared. Because of the symmetry of the LT molecule, there is a unique orientation for fitting the three-dimensional cylindrical CTX map into the three-dimensional LT map. The dimensions measured for CTX were slightly smaller than those of LT. This may represent a real difference, but is most likely due to the shrinkage effects of the negative stain on CTX.

McDaniel and McIntosh (1986) have shown by x-ray diffraction that the head group of G_{M1} extends 21 Å from the hydrocarbon-water interface. As first proposed by Sixma et al. (1992) for LT, this distance is not sufficient for the G_{M1} binding region to face away from the membrane without all of CTA and some of the CTB-pentamer inserting into the bilayer as the toxin binds. Our results show that there is a small but detectable space between the bottom of the CTX toxin and the lipid layer. CTX, therefore, does not appear to be in contact with, or penetrate, the membrane as it binds.

The initial binding orientation of CTX determined from these studies agrees with that reported by Tomasi and Montecucco (1981). Using hydrophobic photolabeling with photoreactive lipids, these investigators reported that only the B and A_2 subunits had contact with the lipid bilayer. Other groups, however, have described results suggesting that the A subunit penetrates the lipid upon binding (Goins and Freire, 1985; Dwyer and Bloomfield, 1982). Previous EM studies of two-dimensional crystals of the CTB-pentamer on monolayers were not able to determine the orientation of the pentamer (Ludwig et al., 1986; Mosser et al., 1992). A three-dimensional map of CTX at 17 Å-resolution indicated that CTA was near the pentamer pore, but the exact location with respect to the membrane was not conclusively determined (Ribi et al., 1988). Our studies provide the first direct visualization of CTX perpendicular to the pore as it binds to a G_{M1}-containing lipid layer, and a schematic diagram of CTX binding is shown in Fig. 4. Combining the binding mechanism proposed here with the A_1-A_2 arrangement in LT, a portion of the A_2 peptide, but none of A_1 may interact with the lipid membrane when the toxin binds. It should be noted that only the initial binding step can be modeled using this system. It is possible that some rearrangement of the toxin takes place shortly after binding especially under conditions favoring the reduction of the A_1-A_2 disulfide bond. A_1 may then be able to insert through the cell membrane and then catalyze the ADP-ribosylation of the α-subunit of G_s. The necessity for toxin internalization, however, with subsequent release of A_1 from an endosomal compartment and transport back to the cell membrane cannot yet be excluded.

We thank Dr. Donald Caspar for use of EM facilities to collect initial data, Dr. John Badger for help with the modeling, and MaryAnn Eastman for technical assistance with the monoclonal antibodies.

This work was supported by grants HL26335 (to G.G.S.) and GM43217 (to G.E.S.) from the National Institutes of Health, and a grant from the Medical Research Council of Canada (to M.R.M.).

REFERENCES

Bernstein, F. C., T. F. Koetzle, G. J. B. Williams, E. F. Meyer, Jr., M. D. Brice, J. R. Rodgers, O. Kennard, T. Shimanouchi, and M. Tasumi. 1977. The protein data bank: a computer-based archival file for macromolecular structures. *J. Mol. Biol.* 112:535–542.

DeWolf, M. J. S., M. Fridkin, and L. D. Kohn. 1981. Tryptophan residues of cholera toxin and its A and B protomers. *J. Biol. Chem.* 256: 5489–5496.

Drew, M. D., A. Estrada-Correa, B. J. Underdown, and M. R. McDermott. 1992. Vaccination by cholera toxin conjugated to a herpes simplex virus type 2 glycoprotein D peptide. *J. Gen. Virol.* 73:2357–2366.

Dwyer, J. D., and V. A. Bloomfield. 1982. Subunit arrangement of cholera toxin in solution and bound to receptor-containing membranes. *Biochemistry*. 21:3227–3231.

Finkelstein, R. A. 1988. Structure of the cholera enterotoxin (choleragen) and the immunologically related ADP-ribosylating heat-labile enterotoxins. *In* Handbook of Natural Toxins, Bacterial Toxins. Vol. 4. M. C. Hardegree and A. T. Tu, editors. Marcel Dekker, New York. 1–38.

Frank, J., M. Rademacher, T. Wagenknecht, and A. Verschoor. 1988. Studying ribosome structure by electron microscopy and computer-image processing. *Methods Enzymol.* 64:3–35.

Frank, J., B. Shimkin, and H. Dowse. 1981. SPIDER—A modular software system for electron image processing. *Ultramicroscopy*. 6:343–358.

Frank, J., A. Verschoor, and T. Wagenknecht. 1985. Computer processing of electron microscopic images of single macromolecules. *In* New Methodologies in Studies of Protein Configuration. T. T. Wu, editor. Van-Nostrand Reinhold, New York. 36–89.

Goins, B., and E. Freire. 1985. Lipid phase separations induced by the association of cholera toxin to phospholipid membranes containing ganglioside G_{M1}. *Biochemistry*. 24:1791–1797.

Janicot, M., F. Fouque, and B. Desbuquois. 1991. Activation of rat liver adenylate cyclase by cholera toxin requires toxin internalization and processing in endosomes. *J. Biol. Chem.* 266:12858–12865.

Jones, T. A. 1978. A graphics model building and refinement system for

macromolecules. *J. Appl. Crystallogr.* 11:268–272.

Ludwig, D. S., R. D. Holmes, and G. K. Schoolnik. 1985. Chemical and immunochemical studies on the receptor binding domain of cholera toxin B subunit. *J. Biol. Chem.* 260:12528–12534.

Ludwig, D. S., H. O. Ribi, G. K. Schoolnik, and R. D. Kornberg. 1986. Two-dimensional crystals of cholera toxin B-subunit-receptor complexes: projected structure at 17 Å resolution. *Proc. Natl. Acad. Sci. USA.* 83:8585–8588.

McDaniel, R. V., and T. J. McIntosh. 1986. X-ray diffraction studies of the cholera toxin receptor, G_{M1}. *Biophys. J.* 49:94–96.

Mosser, G., and A. Brisson. 1991. Conditions of two-dimensional crystallization of cholera toxin B-subunit on lipid films containing ganglioside G_{M1}. *J. Struct. Biol.* 106:191–198.

Mosser, G., V. Mallouh, and A. Brisson. 1992. A 9 Å two-dimensional projected structure of cholera toxin B-subunit-G_{M1} complexes determined by electron crystallography. *J. Mol. Biol.* 226:23–28.

Moss, J., and M. Vaughan. 1988. Cholera toxin and *E. coli* enterotoxins and their mechanisms of action. *In* Handbook of Natural Toxins, Bacterial Toxins. Vol. 4. M. C. Hardegree and A. T. Tu, editors. Marcel Dekker, New York. 39–87.

Reed, R. A., J. Mattai, and G. G. Shipley. 1987. Interaction of cholera toxin with ganglioside G_{M1} receptors in supported lipid monolayers. *Biochemistry.* 26:824–832.

Ribi, H. O., D. S. Ludwig, K. L. Mercer, G. K. Schoolnik, and R. D. Kornberg. 1988. Three-dimensional structure of cholera toxin penetrating a lipid membrane. *Science (Wash. DC).* 239:1272–1276.

Sheriff, S., E. W. Silverton, E. A. Padlan, G. H. Cohen, S. J. Smith-Gill, B. C. Finzel, and D. R. Davies. 1987. Three-dimensional structure of an antibody-antigen complex. *Proc. Natl. Acad. Sci. USA.* 84: 8075–8079.

Sixma, T. K., S. E. Pronk, K. H. Kalk, E. S. Wartna, B. A. M. van Zanten, B. Witholt, and W. G. J. Hol. 1991. Crystal structure of a cholera toxin-related heat-labile enterotoxin from *E. coli*. *Nature (Lond.).* 351:371–377.

Sixma, T. K., S. E. Pronk, K. H. Kalk, B. A. M. van Zanten, A. M. Berghuis, and W. G. J. Hol. 1992. Lactose binding to heat-labile enterotoxin revealed by X-ray crystallography. *Nature (Lond.).* 355:561–564.

Stallmeyer, M. J. B., S.-I. Aizawa, R. M. MacNab, and D. J. DeRosier. 1989. Image reconstruction of the flagellar basal body of *Salmonella typhimurium*. *J. Mol. Biol.* 205:519–528.

Tomasi, M., and C. Montecucco. 1981. Lipid insertion of cholera toxin after binding to G_{M1}-containing liposomes. *J. Biol. Chem.* 256:11177–11181.

Tran, D., J. L. Carpentier, F. Sawano, P. Gorden, and L. Orci. 1987. Ligands internalized through coated or noncoated invaginations follow a common intracellular pathway. *Proc. Natl. Acad. Sci. USA.* 84:7957–7961.

Tsuji, T., T. Honda, T. Miwatani, S. Wakabayashi, and H. Matsubara. 1985. Analysis of receptor-binding site in *Escherichia coli* enterotoxin. *J. Biol. Chem.* 260:8552–8558.

Wisnieski, B. J., and J. S. Bramhall. 1981. Photolabeling of cholera toxin subunits during membrane penetration. *Nature (Lond.).* 289:319–321.